HHS Public Access

Author manuscript

Biomaterials. Author manuscript; available in PMC 2016 August 01.

Published in final edited form as:

Biomaterials. 2015 August ; 59: 30–38. doi:10.1016/j.biomaterials.2015.04.040.

Sample-free quantification of blood biomarkers via laser-treated skin

Bo Li[a,1], **Ji Wang**[a,1], **Seung Yun Yang**[b,c], **Chang Zhou**[a], and **Mei X. Wu**[a,d,*]

[a]Wellman Center for Photomedicine, Massachusetts General Hospital, Department of Dermatology, Harvard Medical School, Boston, Massachusetts, 02114, United States

[b]Division of Biomedical Engineering, Department of Medicine, Brigham and Women's Hospital, Harvard Medical School, Boston, Massachusetts 02115, United States

[d]Harvard-MIT Division of Health Sciences and Technology, Cambridge, Massachusetts 02142, United States

Abstract

Surface modified microneedle (MN) arrays are being developed to capture circulating biomarkers from the skin, but inefficiency and unreliability of the current method limit its clinical applications. We describe here that illumination of a tiny area of the skin with hemoglobin-preferably absorbent laser increased the amount of circulating biomarkers in the upper dermis by more than 1,000-fold. The hemoglobin-specific light altered the permeability of capillaries leading to extravasation of molecules but not blood cells beneath the skin involved. When specific probe-coated MN arrays were applied into the laser-treated skin, the biomarkers accumulated in the upper dermis were reliably, accurately, and sufficiently captured as early as 15 min of the assay. The maximal binding occurred in one hr in a manner independent of penetration depth or a molecular mass of the biomarker. With anti-fluorescein isothiocyanate (FITC)-MNs, we were able to measure blood concentrations of FITC in mice receiving FITC intravenously. The sensitivity and accuracy were comparable to those attained by fluorescence spectrophotometer. Likewise, MNs containing influenza hemagglutinin (HA) could detect anti-HA antibody in mice or swine receiving influenza vaccines as effectively as standard immunoassays. The novel, minimally invasive approach holds great promise for measurement of multiple biomarkers by a single array for point-of-care diagnosis.

[*]Address Correspondence to: Dr. Mei X. Wu, Wellman Center for Photomedicine, Massachusetts General Hospital, 50 Blossom Street, Edwards 222, Boston, MA 02114, TEL: 617-726-1298; FAX: 617-726-1206; mwu5@mgh.harvard.edu.

[c]Current address: Department of Biomaterials Science, Life and Industry Convergence Institute, Pusan National University, Miryang, Gyeongnam 627-706, Republic of Korea.

[1]Contribute equally to this work

The authors have no conflict of interest to declare

Keywords

Sample-free; Microneedles; Laser; and Circulating Biomarkers

1. Introduction

The ability to quantify circulating biomarkers in a timely fashion is crucial for monitoring diseases, organ functions, and drug abuse [1–3], so there have been considerable efforts towards developing more convenient and reliable technologies for measuring blood biomarkers [4–6]. Among the technologies, finger-prick has revolutionized our way to monitor plasma glucose levels in patients with diabetics. However, the technology is highly dependent on readable signals, suitable only for relatively abundant analytes in the serum so far. Most of current methods for measuring circulation biomarkers still rely on blood collection that requires a high level of medical training [7,8], as well as time-consuming, labor-intensive blood sample process, storage, and analysis [9,10]. There are great challenges to develop alternative, rapid, sensitive, and reliable technologies for point-of-care molecular diagnosis.

Recently, microneedle (MN) array-based minimally invasive diagnosis has attracted attention for rapidly detecting blood biomarkers through the skin [4,11,12]. Several surface modified MN arrays have been fabricated, capable of recognizing circulating viral proteins and specific antibodies in mouse dermis, allowing biomarker detection without blood collection and sample processing [13,14]. Unfortunately, such arrays have two key drawbacks. Concentrations of most blood biomarkers in the upper dermis are too low to be captured by MN arrays. Hence, deep dermal penetration and prolonged application are required to surmount this flaw, which is likely to cause pain, compromising patient compliance [11,12]. Secondly, there are unacceptably large variations in probe bindings to individual MNs within the same array, due to uncharacterized leakage of biomarkers through capillaries damaged by penetrating MNs [4,15]. After all, only a few MNs in each array cause such unintended damage and display strong binding, whereas most of the MNs in the array show no or weak capture of plasma biomarkers. Such high variability makes it impossible to quantify multiple biomarkers in one array, or reliably measure a single biomarker for quantity-based diagnosis and/or prognosis.

Consequently, we propose applying laser illumination to both increase overall concentrations of biomarkers in the upper dermis and reduce variability of biomarkers captured on individual MNs in the same array. For decades, lasers have been used to treat vascular malformation in clinics, based on the concept of “selective photothermolysis” [16]. In the treatment, a long pulse 595 nm dye laser at doses of 4~20 J/cm^2 is applied to the skin and excites hemoglobin and oxygenated hemoglobin resulting in heat release that ruptures malformed capillaries in human skin [17]. Abundant hemoglobin and oxygenated hemoglobin are presented within red blood cells and absorb preferably light at a wavelength range of 530–600 nm [18]. We postulate that a much lower energy density of the light can induce transient molecular extravasation of skin capillary at the site of laser illumination. Laser-induced leakage of circulating biomarkers results in their accumulation in the skin permitting highly efficient detection of them by surface modified MNs. The degree and

length of capillary extravasation can be well controlled by laser power, pulse width, and duration of illumination to ensure no tissue injury.

The current investigation shows that safely inducing controllable capillary leakage within the skin requires a 532 nm pulse laser for 5 seconds (s) of illumination in mice, or a pulse 595 nm clinic laser for 0.45 ms in swine [19,20]. The extravasation appears to occur for blood substances or macromolecules, but not for any cells. It is restrained within the site of laser illumination, measurable after one minute and peaking at 10 minutes before subsiding, ultimately resolving in ~2 hr. Concentrations of blood biomarkers rise by more than 1,000-fold in the upper dermis. Application of probe-coated MNs into the laser-treated site could reliably, accurately, and sufficiently quantify blood biomarkers in a manner independent of penetration depth or a molecular mass of the biomarker.

2. Materials and methods

2.1 Materials

A heterobifunctional polyethylene glycol linker of 5 kDa, referred to as COOH-PEG-SH, was purchased from JenKem Technology (Allen, TX, USA); 1-Ethyl-3-(3-dimethylamino-propyl) carbodiimide (EDC), N-hydroxysuccinimide (NHS), fluorescein isothiocyanate (FITC), gold chloride trihydrate, and ovalbumin (OVA) from Sigma-Aldrich; and sylgard 184 elastomer from Dow Corning (Midland, MI, USA). Influenza hemagglutinin (HA) protein from A/PR/8/34 strain was obtained from BEI resources, SU-8 2150 epoxy-based negative photoresist from MicroChem (Newton, MA, USA), and polyclonal rabbit anti-FITC antibody and normal control rabbit IgG from Life Technologies (Frederick, MD, USA). FITC-conjugated secondary antibodies against mouse IgG or pig IgG were acquired from BioLegend (San Diego, CA, USA) or Sigma (St Louis, MO, USA) respectively. Inactivated influenza vaccine was made by treatment of purified A/PR/8/34 virus with 0.024% formaldehyde at 4 °C for one week as previously described [21]. The amount of HA protein in the vaccine was quantified by SDS-PAGE following a standard procedure.

2.2 Fabrication and characterization of MNs

A female MNs mold was fabricated using a soft lithographic process. Briefly, a 1 mm thick SU-8 layer was spin-coated onto a freshly treated Si wafer, baked for 10 hr, and then exposed to ultraviolet light (365 nm, 10 W/cm^2) at an angle of 20° and 10 rpm for 600s through the dots patterning photomask that was placed on the surface of light-sensitive SU-8 layer, followed by baking for 2 hr [22]. A female MNs mold was formed after developing the SU-8 mold in propylene glycol methyl ether acetate for 6 hr. To increase surface hydrophobicity of the conical cavities, trichloro (1H, 1H, 2H, 2H-perfluorooctyl) silane or fluorosilane was gas-phase deposited onto the surface. The base and curing agent of PDMS were then mixed at a ratio of 1:10 and cast into the SU-8 mold. After being de-gassed and cured at 95 °C, the newly formed PDMS MN array was peeled off, treated with fluorosilane again, and used to generate another female PDMS MNs mold following a similar procedure. The second female MNs mold was cast with biocompatible epoxy-based resin, creating MNs with greater mechanical strength than PDMS MNs. MN arrays with 30 μm and 100 μm in lengths for mice or 250 μm and 500 μm for pigs were fabricated similarly. The resultant

MNs were sprayed with chrome, forming a 20 nm adhesion layer on which 100 nm gold was coated as described [11]. The heterobifunctional linker COOH-PEG-SH was immobilized on the surface of gold-coated MNs via its SH group per the manufacturer's instruction [12]. The linker not only reduced non-specific binding but also provided an anchor for capturing biomarkers. Rabbit anti-FITC or control antibody at 10 μg/mL, or HA or ovalbumin protein at 100 μg/mL, was used to covalently attach to the COOH of the linker in a standard EDC/NHS chemical reaction. The resultant MNs were rinsed 3 times with 0.05% Tween-20 in PBS to remove non-covalently bound antibodies or proteins and stored at 4 °C in PBS [13,14].

2.3 Specific binding and quantification of the modified MNs

MN arrays coated with rabbit anti-FITC or control antibody were incubated with skimmed milk at 36 °C for 1 hr to block non-specific binding, and then washed three times each for 1 min. The antibody-coated MN arrays were incubated at 36 °C with varying concentrations of FITC in 2 % bovine serum albumin (BSA) in PBS (pH 6.8) for 2 hr, or 2.5 μM FITC for indicated times. Photos of resulting MN arrays were captured by fluorescence microscopy, and the fluorescence intensity on each MN was analyzed by image J software [14]. In a separate study, sera were prepared from naive mice or mice immunized intramuscularly with 50 μl inactivated influenza vaccine (1 μg HA/mouse) for 4 weeks. HA-MNs, OVA-MNs, or uncoated MNs were immersed for 30 min at 1:300 dilutions for immunized serum or 1:100 for serum from naive mice. After thorough washing, the MNs were incubated with FITC-conjugated anti-mouse IgG and FITC intensities of individual MNs were measured as above. The amount of anti-HA IgG captured on the MNs was estimated by a standard curve run in parallel. The animals were housed in the specific pathogen-free animal facilities of Massachusetts General Hospital (MGH). All animal experiments were reviewed and approved by the MGH Institutional Animal Care and Use Committee.

2.4 Laser-induced extravasation in the skin

To enhance circulating biomarkers in the upper dermis or epidermis, about 1 cm^2 of the lower dorsal skin of Balb/c mice (Charles River Laboratories, Wilmington, MA) was hair removed and illuminated the next day by a 532 nm pulse Nd:YAG laser with a beam diameter 7 mm, pulse width 7 ns, at a fluence of 0.5 J/cm^2 (UP-6G model, RMI Laser, LLC). FITC or Evans blue dye at indicated amounts was intravenously administered via a tail vein prior laser illumination. Extravasation of FITC or Evans blue dye at laser-treated site was tracked by intravital two photon confocal microscopy (Olympus FV-1000) before laser illumination and at varying times afterwards. The skin tissue samples were also harvested for standard hematoxylin and eosin staining and histological evaluation, for fluorescence intensity measurement after cryosectioning, or for extraction of Evans blue dye. To study laser-induced extravasation in pigs, male Yorkshire pigs at 4 months of age and about 30 kg were obtained from the Teaching and Research Resources at Tufts University. The lower dorsal skin of the pigs was illuminated with a clinical, long pulse 595 nm laser with a beam diameter 7 mm, pulse width 0.45 ms, at a fluence of 4 J/cm^2 after 20 mL Evans blue dye at 2 mg/mL was i.v. administered via an auricular vein. Evans blue dye leakage in the skin was visualized by naked eye and skin photos were taken at indicated

times after laser treatment to assess skin reaction and leakage of Evans blue dye at laser-treated sites.

2.5 Measurement of circulating biomarkers

To capture circulating FITC in the skin, Balb/c mice were i.v. injected with varying amounts of FITC, followed by laser illumination of the site of MN array application as above. Anti-FITC or control antibody-coated MNs were applied into laser-treated site or non-laser treated site for indicated times, after which the patches were removed, washed, and analyzed as above. Similarly, HA-MNs and OVA-MNs with two different lengths were applied into skin treated with either laser or sham light as above in mice that had received inactivated influenza vaccine 4 weeks ago. After 30 min application in the skin, the MN patches were carefully removed, transferred to a 96-well plate, and washed thoroughly. To the MNs-containing plates, FITC-conjugated secondary antibody was added and incubated for an additional hour at room temperature, followed by washes. FITC intensity on each MN in the array was analyzed as above. Measurement of circulating anti-HA IgG in pigs was conducted similarly except that patches containing longer MNs, 250 μm and 500 μm, were employed in the skin for only 15 min. Two weeks before testing, the pigs were immunized with inactivated influenza vaccine at a dose of 2 μg HA/pig via intradermal injection. The amount of anti-HA IgG captured on the MNs was quantified on the basis of a standard curve generated by immunofluorescence (IF) assays of purified anti-HA antibody. The amounts of anti-HA IgG in the circulation was calculated by a formula: the amount of anti-HA IgG on the MNs ÷ skin tissue weight × a tissue dilution factor that was 10.9 in mice or 15.7 in pigs, corresponding to a difference in Evans blue concentrations between laser-treated skin and blood.

2.6 Immunofluorescence (IF) assays

For quantification of anti-HA IgG, anti-HA IgG antibody was first purified from immunized pigs or mice as a standard. To purify the protein, sera were collected from the animals and passed through an HA protein affinity column that was made by a covalent linkage of HA's COOH group with the activated NHS in agarose resin (Thermo Pierce) in a standard EDC/NHS chemical reaction. The purity of the resultant anti-HA IgG was verified by SDS-PAGE and the amount of purified anti-HA IgG was quantified in the basis of the absorbance at 280 nm and stored at 4 °C [23]. The anti-HA IgG standard at a series of dilutions, along with immunized and control sera diluted similarly, were added in triplicate into a high protein binding black 96-well plate with clear flat bottom, which had been coated with HA protein overnight at 4 °C. The resultant plate was incubated with skimmed milk for 1 hr, and then with FITC-conjugated anti-mouse or pig IgG. Fluorescence intensity in each well was measured by fluorescence microplate reader after washes. The amount of anti-HA IgG in the serum was determined based on FITC intensity and the standard curve. Serum of immunized pigs or mice was collected just before the MNs were applied into the skin. Control serum was collected prior immunization.

2.7 Statistical analysis

The difference between two groups was analysed by two tailed t-test. One way ANOVA was used among multiple groups. P value was calculated by PRISM software (GraphPad, CA) and the statistical significance is indicated by * $P < 0.05$, ** $P < 0.01$ and *** $P < 0.001$.

3. Results and Discussion

3.1 FITC capture by anti-FITC antibody coated MNs

Anti-FITC antibody coated MNs (anti-FITC-MNs) and control antibody coated MNs (C-MNs) were prepared in arrays that each included 9 MNs as reported [22,24]. They were then incubated with FITC at concentrations ranging from 0.25 to 25 μM for 2 hr at 36 °C, a temperature corresponding to that of skin. Photos of resulting MNs under a fluorescence microscope confirmed specific FITC binding of the MNs (Fig. 1A), as fluorescence was uniformly presented on anti-FITC-MNs but not on C-MNs. The fluorescence intensity of each MN was then quantified by Image J, and a mean intensity of each array was correlated to FITC concentrations (Fig. 1B). The intensity also increased proportionally to length of incubation (Fig. 1C).

When 100 μm MNs were inserted into the dorsal skin of mice receiving 100 μL FITC at 4 mg/mL, no C-MN arrays reached fluorescent intensity above the cutoff line after two hours in the skin (Fig. 1D). On the other hand, a few anti-FITC-MN arrays exceeded the cutoff value after 30 min, but the mean intensity did not exceed cutoff until 1 hr into the experiment (Fig. 1D), and even then statistical analysis indicated an insignificant difference in the intensity between control and anti-FITC-MN arrays. Thus, by this method anti-FITC-MNs only captured FITC above background at a statistically significant level by the 2 hr mark. (Fig. 1D). Yet, there were large variations in intensity by this point, such that only 5 of 10 arrays were above the cutoff line. These variations apparently resulted from FITC unevenly captured on some MNs in the array. Among the 9 MNs in the inset of Figure 1D, 2 MNs displayed strong FITC binding, 3 had weak interactions, and 4 exhibited no FITC binding at all. The uneven FITC binding was presumably caused by uncharacterized capillary damage around individual MNs during MN penetration, since in vitro assays confirm a uniform FITC binding in all MNs in the array (Fig. 1A). As depicted in Figure 7B, high FITC binding may occur only on a MN that is physically at or close to the site of capillary damage such as MN#1, but not on a MN that is physically away from the site such as MN#3. The insensitivity, high variations, and long duration of the assay must be adequately addressed before it can be advanced to the clinics. Uniform and strong accumulation of blood biomarkers within the skin at the site of MN insertion is a prerequisite to reliable diagnosis with MNs-based arrays.

3.2 Laser induces controllable extravasation

Having conducted a series of pilot studies with various lasers at different energy densities, we found that a 532 nm pulse Nd:YAG laser (NYL) could trigger extravasation of the capillary beneath the skin after 5s illumination, without incurring any damage to the surrounding tissues. Briefly, the lower dorsal skin of mice was hair removed and illuminated by NYL laser for 5s with a beam diameter 7 mm and pulse width 7 ns at 0.5 J/cm^2 after

intravenous injection with 100 μL FITC at 4 mg/mL. The illumination site was subjected to analysis with two photo confocal laser scanning microscopy at indicated times. Prior laser illumination, capillary network was clearly visible by fluorescent labeling, as FITC was well confined within the microvessels on a high magnification (Fig. 2A, the upper left in the first panel). Upon illumination, FITC leakage was seen immediately, quickly accumulating in the skin tissue within 1 min (Fig. 2A), reaching a maximal level in 10 min. The strong fluorescence was sustained for 10~20 min, subsided gradually thereafter, diminished substantially in 1 hr, and completely disappeared in 2 hr (Fig. 2A). We also verified laser-induced capillary permeability using Evans blue dye, which binds albumin in the bloodstream and becomes impermeable to blood vessels after intravenous injection [25,26]. Evans blue could be seen in the skin immediately after laser illumination by naked eye, reached a maximal level in 15 min, and completely resolved in 2 hr. Besides its visible blue color, Evans blue is also a red fluorescent dye with an excitation at 620 nm and emission at 680 nm [26]. Under a fluorescent microscope, Evans red fluorescence was seen throughout the dermis, and in particular a bright fluorescence was presented in the upper dermis in laser-treated skin, in marked contrast to non-laser-treated skin where there was dim fluorescence in the dermis and little in the supper dermis (Fig. 2B). The fluorescence intensity in the upper dermis was more than 1,000-fold higher in the presence than in the absence of laser illumination as analyzed by Image J (Fig. 2C). When laser-treated skin with dimensions of 5×5 mm^2 and 500 μm depth was dissected 10 min after illumination, Evans blue was extracted from the skin and measured by fluorescence spectrophotometer, yielding 7.3 μg/mL of the dye in the skin. In comparison to a concentration in serum (80.1 μg/mL), Evans blue was diluted by ~11-fold in skin tissue. The factor of skin tissue dilution was subsequently used to calibrate skin measurement of blood biomarkers. Likewise, we determined a tissue dilution factor of 3 for FITC under similar laser treatment, much less than Evans blue-albumin, probably because the smaller size of FITCs allows for rapid diffusion from vessels and accumulation in the skin. The data suggests that a tissue dilution factor must be taken into consideration when a biomarker detected in the skin is correlated with its blood concentration. As a final remark, while inducing significant extravasation, no significant alteration was found histologically in laser-treated skin as compared to non-laser-treated control, except for slight capillary dilation in laser-treated skin (Fig. 2D).

The high level and even accumulation of circulating biomarkers in the skin after laser illumination should result in robust improvement of MNs-based assays. To test this, mice receiving 100 μL FITC at 4 mg/mL were treated with laser as above, followed by application of anti-FITC-MN or C-MN patch into laser-treated skin. The patches were removed at indicated times and FITC intensities were measured as Fig. 1D. As can be seen in Fig. 3A, only one or two C-MN arrays among 10 arrays tested demonstrated FITC signal barely reaching or above the cutoff level in one or two hr assays. In comparison, FITC could be significantly detected by anti-FITC-MNs as early as 15 min into the assay ($P < 0.05$). Extending a duration to 30 min raised the level of FITC detection 3-fold greater than the cutoff value ($P < 0.01$). An additional 2-fold increase in FITC capture on anti-FITC-MNs was achieved by prolonging the application time from 30 min to 1 hr ($P < 0.001$), and no further increment was attained by extending to 2 hr from 1 hr application (Fig. 3A). This peaking time is only 1/6 of that reported in previous investigation [4]. A markedly shortened

time of detection, from 4~6 hr to 30 min, confers great potentials for point-of-care diagnosis and onsite monitoring of biological states. Moreover, the lack of an increase in specific binding after prolonged insertion can minimize false positives from unintentionally extending insertions into the skin. In addition, the level of FITC captured on the array was 5-fold greater in the presence than in the absence of laser treatment, comparable to that obtained in standard immunofluorescence assays run in parallel. Most importantly, FITC captured on each array did not differ significantly among the ten arrays tested at different times (Fig. 3A), profoundly improving the reliability of the assay. The deviation was 13.57, which was in a range of conventional immunofluorescence assays (9.45). Meanwhile, experimental error in the absence of laser treatment was 88.21, 6.5 times higher and unacceptable for clinical diagnosis. In marked contrast to the uneven signals appearing on anti-FITC-MNs in a similar array when inserted into non-laser-treated skin (Fig. 1D, inset), photographs indicated strong and uniform FITC signals presented on all anti-FITC-MNs in each array (Fig. 3A, inset). This uniform binding of FITC on each MN is a prerequisite to detecting multiple biomarkers in a single array, a technology that is long sought after in today's medicine. Furthermore, because the MNs reach only the upper dermis through the epidermis, the patch application should be painless as there are few nerves in the upper dermis or the epidermis. Thus, laser treatment of a tiny area of the skin safely and conveniently offers the following advantages: 1. greatly enhancing the sensitivity of MNs-based arrays as a result of vigorous accumulation of circulating biomarkers in the upper dermis; 2. substantially reducing the measurement error from one test to another, making the assay highly reliable for diagnosis; 3. allowing uniform capture on each MN in the same array and thus making it possible to accurately detect multiple biomarkers in a single patch; and 4. minimally invasive and painless.

To correlate fluorescence intensity on anti-FITC MNs to FITC concentrations in circulation, FITC at different concentrations was i.v. administered into the separate groups of mice, followed by insertion of C-MNs and anti-FITC-MNs into the different sites of laser illumination for 30 min as above; meanwhile, a small blood sample was taken from each mouse via its tail vein immediately after MN patch application. Plasma was prepared from the blood by centrifugation at 1,000 g for 10 min, followed by filtering through a membrane with 10,000 MW cutoff. The resultant FITC concentrations in the ultrafiltrates were determined by fluorescence spectrophotometer, which is commonly used to measure FITC in serum samples. FITC concentrations in the blood were 29 ± 6.8, 209 ± 13, 2,313 ± 48, and 4,022 ± 75 ng/mL corresponding to i.v. injections of 100 μL FITC at 0.4, 4, 40, and 80 mg/mL, respectively. The amounts of FITC detected by anti-FITC-MNs were 237 ± 32, 2,778 ± 114, and 3,703 ± 89 ng/mL for mice receiving 100 μL FITC at 4, 40, and 80 mg/mL, after normalization with a tissue dilution factor 3 mentioned above. Thus, FITC concentrations measured via serum samples and MNs yielded remarkably close results (Fig. 3B). The FITC level was undetectable by MNs in mice i.v. injected with 0.4 mg/mL of FITC (Fig. 3B). We conclude that surface modified MN arrays can accurately measure small biomarkers in circulation if laser is pre-applied to the site of MN insertion.

3.3 Measurement of anti-HA IgG in immunized mice

Small biomarkers differ from macromolecules in terms of leakage, diffusion, binding dynamics from dermal capillary to perivascular skin tissue, and FITC injected may also differ from natural biomarkers. We thus tested whether this novel approach could measure clinically relevant macromolecules as sufficiently as FITC. To this end, influenza hemagglutinin (HA) protein or control ovalbumin (OVA) was mounted on MNs to generate HA-MNs and OVA-MNs arrays as described [11,12]. The specificity and sensitivity of resultant MN arrays were verified by incubation of the array for 30 min with 1:300 diluted serum prepared from immunized mice or 1:100 from control mice, and then with FITC-conjugated secondary antibody (Fig. 4A). Strong fluorescence signal was seen only on HA-MNs incubated with serum of immunized mice, not naive mice. No positive FITC binding was detected over background either on uncoated MNs or OVA-MN controls irrespective of the serum incubated with, confirming specific binding of anti-HA antibody on HA-MNs. Moreover, with known concentrations of anti-HA IgG, HA-MNs were confirmed to be able to measure anti-HA IgG at a concentration as low as 50 ng/mL in proportional correlation with anti-HA IgG concentrations in a range from 50 to 250 ng/mL (Fig. 4B).

HA-MNs and OVA-MNs of 30 μm and 100 μm in length were then employed to capture anti-HA IgG in the upper or deep dermis, respectively, in mice that received influenza vaccines 4 weeks prior. Out of 6 HA-MNs at 100 μm length, 4 could capture anti-HA IgG above the cutoff value from deep dermis after 30 min insertion ($P < 0.05$), but the 30 μm HA-MNs did not capture anti-HA IgG above the cutoff level with statistical significance (Fig. 4C). These observations are in agreement with previous investigations showing that the amount of blood biomarkers captured by MNs increased with the penetration depth and time [4,27]. As the dermis contains nerves and touch receptors, insertion of MNs into the dermis is expected to bring about significant pain. Moreover, longer MNs are relatively easier to break than shorter MNs upon insertion, which may cause unwanted adverse events. These adverse events were effectively circumvented with laser treatment that enabled 30 μm HA-MNs to capture anti-HA IgG at levels 4-time greater than the cutoff level in the upper dermis (Fig. 4C, $P < 0.001$). Interestingly, there was no difference in specific antibody binding between 30 and 100 μm HA-MNs in the presence of laser illumination, confirming uniform distribution of anti-HA IgG throughout the dermis as shown in Figure 2B. This is of highly clinical significance if the amount of IgG measured by the assay is independent on the depth of MNs or a longer time of the insertion. It can be envisioned that potential errors of the measurement would arise substantially when MN arrays are applied by different people at various places where time of insertion may not be well controlled and the force of insertion of the patch may vary from one person to the other. These errors would be eliminated effectively if laser pre-illumination is applied to the site of MNs application as demonstrated in this study. In parallel, OVA-MNs were negative irrespective of the MN length or in the presence or absence of laser treatment (Fig. 4C and data not shown). The amount of anti-HA IgG measured on HA-MNs was 235 ± 21 ng/mL based on the standard curve (Fig. 4B). The blood concentration would be ~11 times higher than this number after calibration by the factor of skin tissue dilution, which was estimated in the basis of Evans blue dilution in the skin mentioned above. The result was strikingly close to the 2.31 ± 0.14 μg/mL obtained by a traditional IF assay of the sample run at the same time (Fig. 4D).

Finally, the deviations of 30 and 100 μm HA-MNs with laser treatment were 0.21 and 0.33, respectively, which were similar to a traditional IF assay that was about 0.14 in parallel tests. In comparison with a deviation of 0.95 in MNs-based analysis alone, a greater than 4-fold precision increase was achieved by simple and brief laser irradiation.

3.4 Measurement of anti-HA IgG in immunized swine

The skin of swine is anatomically and physiologically more similar to that of humans than mice. We went on to validate the assay in pigs receiving influenza vaccines in order to determine its clinical potential. A clinical, long pulse 595 nm laser was used to illuminate the site of HA-MN array application because of its common use in humans [28]. The power used in clinic was 7.5~20 J/cm^2 and we thus tried the energy downward as we had no intention to rupture any vessels. Prior to laser illumination, Evans blue dye at 20 mg/mL and 20 mL per pig was intravenously administered before different sites of the pig skin were illuminated with the laser at varying energy densities from 7 to 4 J/cm^2. Ten minutes after laser illumination, a significant amount of Evans blue dye could be seen by naked eyes (Fig. 5A). To our surprise, Evans blue extravasation appeared not to arise with increasing density of laser energy but skin injury did. We therefore chose the lowest energy density 4 J/cm^2 of the laser device, which was a half of the lowest laser energy used in clinics. Similar to what was described in mice, the laser setting resulted in a strong and uniform distribution of Evans blue fluorescence in the upper dermis, contrasting that of skin from the same pigs un-treated by laser (Fig. 5B). The increment in fluorescence intensity in the upper dermis was about 1,000-fold higher than controls (Fig. 5C). To determine the tissue dilution factor, Evans blue was extracted from the skin of 5×5 mm^2, 2 mm depth and the amount in laser-treated skin was about 5.7 μg/mL as determined by fluorescence spectrophotometer, which was 15.7 times lower than that in serum. The greater dilution factor compared to that in mice may be associated with the laser and size of the body or velocity of the blood in pigs. As for skin reaction, we observed skin redness 1 min after the illumination, which peaked at 10 min, but subsided gradually thereafter and completely normalized within 2 hr of laser illumination (Fig. 5D). Clinical description of pain levels with 7.5 J/cm^2 is about 1~2 and the pain induced by 4 J/cm^2 should be less than that.

We fabricated 250 and 500 μm HA-MNs and OVA-MNs to accommodate the thicker skin of pigs and verified their specificity similarly as described in the mouse study (Fig. 4A). The HA-MNs penetrated either directly into upper dermis or dermis of pigs receiving influenza vaccines two weeks ago or into the site of laser illumination in the same pigs. In the absence of laser illumination, 250 μm HA-MNs failed to capture a significant amount of anti-HA IgG over background after 15 min application (Fig. 6A). Although 500 μm HA-MNs could detect anti-HA IgG above the cutoff level under a similar condition, the results were inconsistent among different arrays (Fig. 6A). In contrast, in the presence of laser illumination, anti-HA IgG was strongly and consistently detected by all HA-MNs at a length of either 250 or 500 μm for only 15 min application (Fig. 6B). The anti-HA IgG level was increased by more than 3-fold in the presence vs. the absence of laser illumination. MNs of 250 μm in length reach only the upper dermis and are considered minimally invasive and painless in swine.

Based on FITC intensity and the standard curve using anti-HA IgG purified from immunized pigs, the amount of anti-HA IgG in the serum was 3.1 ± 0.067 μg/mL when measured by traditional IF assays, which was very close to 3.2 ± 0.17 and 3.1 ± 0.16 μg/mL, respectively, obtained by 250 or 500 μm HA-MNs at the site of laser illumination after normalization with a tissue dilution factor. More importantly, the deviations were 0.47 for 250 μm HA-MNs or 0.82 for 500 μm HA-MNs, respectively, in the absence of laser treatment, which were much larger than 0.12 obtained in the presence of laser illumination. The data confirm that a clinical 595 nm dye laser could greatly improve accuracy, reliability, and sensitivity of MNs-based quantification of circulating biomarkers via the skin of pigs.

4. Conclusions

We showed for the first time that surface modified MN-arrays could accurately, reliably, and quickly quantify circulating biomarkers in the upper dermis after laser treatment. Significant and transient extravasation of blood biomarkers could be safely achieved by brief laser irradiation of the MN array application site. The assay is independent of the length of the MNs or a molecular mass of the biomarkers as a small model molecule FITC and a macromolecule IgG can both be measured sufficiently by this minimally invasive procedure. More studies should be carried out to determine how tissue dilution factors may be related to body weight and laser specifications, or whether a reference molecule should be included in the same array to further minimize the variations from person to person. However, considering the huge difference in body weight between pigs and mice (2,000-fold), the difference in a tissue dilution factor is rather small, only ~30% (11 vs 16) between the two species. The difference from person to person may be neglected or considered only when large scale differences exist such as that between infants and adults, or persons with a body weight differing drastically from a normal range. In the future, a handheld device can be engineered to incorporate laser illumination, an applicator for MN arrays, and record of fluorescence intensity in a single device for convenient detections of multiple blood biomarkers in one array, which would have a tremendous impact on healthcare.

Acknowledgments

This work was supported by the National Institutes of Health grants AI089779, AI070785, AI097696, and DA028378 (to M.X.W.). The authors would like to thank Prof. Jeffrey M. Karp at Brigham and Women's Hospital, Harvard Medical School and the Center for Nanoscale Systems at Harvard University for their help in fabricating microneedle patches. The authors are also grateful to Jeffrey H. Wu for his editing and to the Photopathology Core at Wellman Center for Photomedicine in Massachusetts General Hospital for their microscopy services.

References

1. Vives-Pi M, Takasawa S, Pujol-Autonell I, Planas R, Cabre E, Ojanguren I, et al. Biomarkers for diagnosis and monitoring of celiac disease. J Clin Gastroenterol. 2013; 47:308–313. [PubMed: 23388848]
2. Donovan DM, Bigelow GE, Brigham GS, Carroll KM, Cohen AJ, Gardin JG, et al. Primary outcome indices in illicit drug dependence treatment research: systematic approach to selection and measurement of drug use end-points in clinical trials. Addiction. 2012; 107:694–708. [PubMed: 21781202]
3. Caccialanza R, Palladini G, Klersy C, Cereda E, Bonardi C, Quarleri L, et al. Serum prealbumin: an independent marker of short-term energy intake in the presence of multiple-organ disease involvement. Nutrition. 2013; 29:580–582. [PubMed: 23298969]

4. Coffey JW, Corrie SR, Kendall MA. Early circulating biomarker detection using a wearable microprojection array skin patch. Biomaterials. 2013; 34:9572–9583. [PubMed: 24044999]
5. Song Y, Zhang Y, Bernard PE, Reuben JM, Ueno NT, Arlinghaus RB, et al. Multiplexed volumetric bar-chart chip for point-of-care diagnostics. Nat Commun. 2012; 3:1283. [PubMed: 23250413]
6. Song Y, Huang YY, Liu X, Zhang X, Ferrari M, Qin L. Point-of-care technologies for molecular diagnostics using a drop of blood. Trends Biotechnol. 2014; 32:132–139. [PubMed: 24525172]
7. Melkie M, Girma A, Tsalla T. The practice of venous blood collection among laboratory and non-laboratory professionals working in Ethiopian Government Hospitals: a comparative study. BMC Health Serv Res. 2014; 14:88–6963-14-88. [PubMed: 24568673]
8. Anderson NL. The clinical plasma proteome: a survey of clinical assays for proteins in plasma and serum. Clin Chem. 2010; 56:177–185. [PubMed: 19884488]
9. Anderson NL. Counting the proteins in plasma. Clin Chem. 2010; 56:1775–1776. [PubMed: 20729300]
10. Jones A, Heyes J. Processing, testing and selecting blood components. Nurs Times. 2014; 110:20–22. [PubMed: 25318151]
11. Jin J, Reese V, Coler R, Carter D, Rolandi M. Chitin microneedles for an easy-to-use tuberculosis skin test. Adv Healthc Mater. 2014; 3:349–353. [PubMed: 23983170]
12. Muller DA, Corrie SR, Coffey J, Young PR, Kendall MA. Surface modified microprojection arrays for the selective extraction of the dengue virus NS1 protein as a marker for disease. Anal Chem. 2012; 84:3262–3268. [PubMed: 22424552]
13. Yeow B, Coffey JW, Muller DA, Grondahl L, Kendall MA, Corrie SR. Surface modification and characterization of polycarbonate microdevices for capture of circulating biomarkers, both in vitro and in vivo. Anal Chem. 2013; 85:10196–10204. [PubMed: 24083844]
14. Corrie SR, Fernando GJ, Crichton ML, Brunck ME, Anderson CD, Kendall MA. Surface-modified microprojection arrays for intradermal biomarker capture, with low non-specific protein binding. Lab Chip. 2010; 10:2655–2658. [PubMed: 20820632]
15. Bhargav A, Muller DA, Kendall MA, Corrie SR. Surface modifications of microprojection arrays for improved biomarker capture in the skin of live mice. ACS Appl Mater Interfaces. 2012; 4:2483–2489. [PubMed: 22404111]
16. Anderson RR, Farinelli W, Laubach H, Manstein D, Yaroslavsky AN, Gubeli J 3rd, et al. Selective photothermolysis of lipid-rich tissues: a free electron laser study. Lasers Surg Med. 2006; 38:913–919. [PubMed: 17163478]
17. Garden JM, Tan OT, Kerschmann R, Boll J, Furumoto H, Anderson RR, et al. Effect of dye laser pulse duration on selective cutaneous vascular injury. J Invest Dermatol. 1986; 87:653–657. [PubMed: 3772159]
18. Anderson RR. Lasers in dermatology--a critical update. J Dermatol. 2000; 27:700–705. [PubMed: 11138535]
19. Broadhurst MS, Akst LM, Burns JA, Kobler JB, Heaton JT, Anderson RR, et al. Effects of 532 nm pulsed-KTP laser parameters on vessel ablation in the avian chorioallantoic membrane: implications for vocal fold mucosa. Laryngoscope. 2007; 117:220–225. [PubMed: 17204988]
20. Rubin IK, Farinelli WA, Doukas A, Anderson RR. Optimal wavelengths for vein-selective photothermolysis. Lasers Surg Med. 2012; 44:152–157. [PubMed: 22241659]
21. Wang J, Li B, Wu MX. Effective and lesion-free cutaneous influenza vaccination. Proc Natl Acad Sci U S A. 2015
22. Yang SY, O'Cearbhaill ED, Sisk GC, Park KM, Cho WK, Villiger M, et al. A bio-inspired swellable microneedle adhesive for mechanical interlocking with tissue. Nat Commun. 2013; 4:1702. [PubMed: 23591869]
23. Wang J, Tong P, Lu L, Zhou L, Xu L, Jiang S, et al. HIV-1 gp41 core with exposed membrane-proximal external region inducing broad HIV-1 neutralizing antibodies. PLoS One. 2011; 6:e18233. [PubMed: 21483871]
24. Xiang Z, Wang H, Pant A, Pastorin G, Lee C. Development of vertical SU-8 microneedles for transdermal drug delivery by double drawing lithography technology. Biomicrofluidics. 2013; 7:66501. [PubMed: 24396551]

25. Radu M, Chernoff J. An in vivo assay to test blood vessel permeability. J Vis Exp. 2013; (73):e50062–e50062. [PubMed: 23524912]

26. Saria A, Lundberg JM. Evans blue fluorescence: quantitative and morphological evaluation of vascular permeability in animal tissues. J Neurosci Methods. 1983; 8:41–49. [PubMed: 6876872]

27. Raphael AP, Meliga SC, Chen X, Fernando GJ, Flaim C, Kendall MA. Depth-resolved characterization of diffusion properties within and across minimally-perturbed skin layers. J Control Release. 2013; 166:87–94. [PubMed: 23266447]

28. Uebelhoer NS, Bogle MA, Stewart B, Arndt KA, Dover JS. A split-face comparison study of pulsed 532-nm KTP laser and 595-nm pulsed dye laser in the treatment of facial telangiectasias and diffuse telangiectatic facial erythema. Dermatol Surg. 2007; 33:441–448. [PubMed: 17430378]

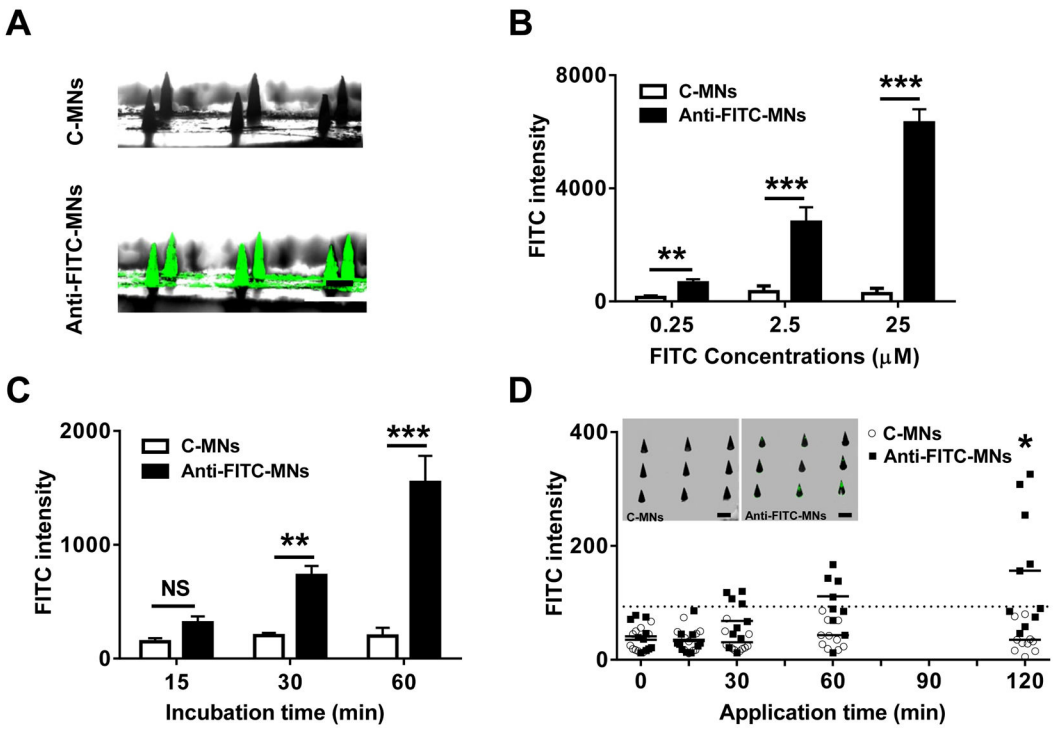

Fig. 1.

FITC measurement *in vitro* and *in vivo* by anti-FITC MNs. (A) Fluorescence images of anti-FITC-MNs and C-MNs. The MNs were incubated with 2.5 μM FITC in 2% BSA solution at 36 °C for 2 hr and photographed by fluorescent microscopy. FITC intensity consistently displays binding to anti-FITC-MNs but not C-MNs when concentration (B) or incubation time (C) is varied. n=6. (D) Detection of circulating FITC *in vivo*. FITC was i.v administered into mice, after which C-MNs (unfilled circle) and anti-FITC-MNs (filled square) were applied into the dorsal skin of the mice. The patches were removed at indicated times and fluorescence intensity in each array was determined. Each symbol represents one array containing 9 MNs, and a dashed horizontal line is a cutoff value for positive FITC binding on the array, which is defined as the mean value of c-MNs plus 3× standard deviation. Insets in (D) show fluorescence images of one C-MN array (left) and one anti-FITC array (right). Note that only 2 out of 9 MNs show significant FITC binding in anti-FITC MNs. Scale=100 μm.

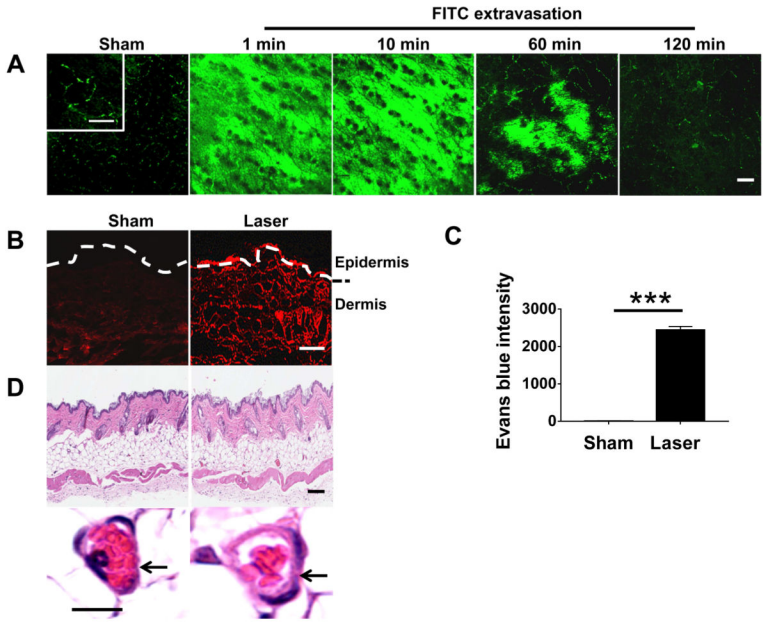

Fig. 2.

Laser induces extravasation. (A) FITC extravasation occurs rapidly in the skin illuminated by 532 nm NYL laser with a fluence of 0.5 J/cm^2. Intravital laser confocal microscopy was used to track FITC signal over time after laser illumination in the skin of mice that had received FITC intravenously. Control skin was shown after illumination with sham light in the same mice. (B) Diffusion of Evans blue dye throughout the dermis after laser illumination. (C) Evans blue intensity increases in upper dermis by more than 1000 times in laser-treated skin as compared with non-laser-treated skin. (D) Histological analysis of control and laser-treated skin. Arrows indicate a capillary vessel. Scale=200 μm in (A), 50 μm in (B), 100 μm in (D, upper) or 5 μm in (D, bottom).

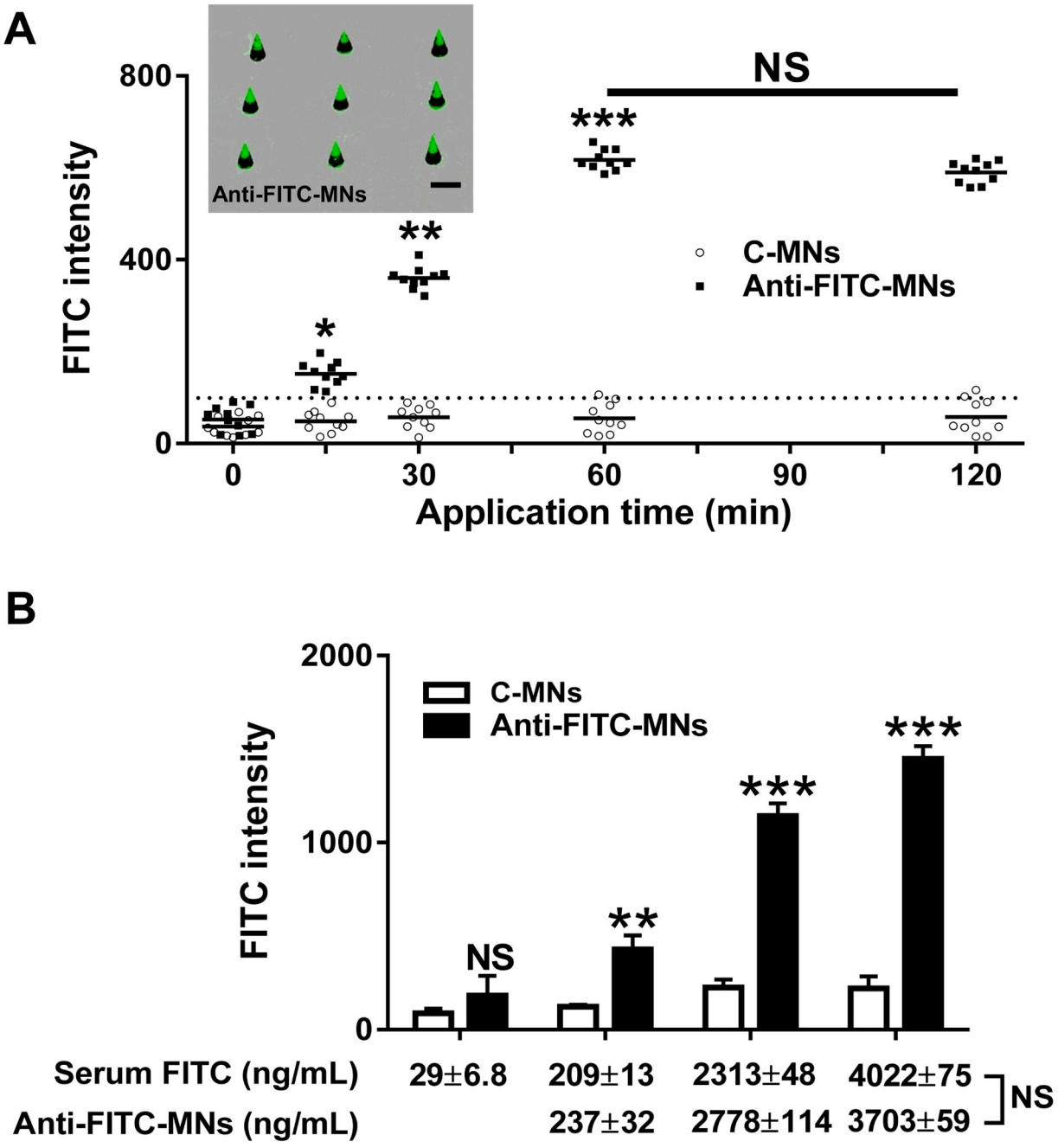

Fig. 3.

Quantification of circulating FITC by anti-FITC-MNs in laser-treated skin. (A) C-MNs (unfilled circle) and anti-FITC-MNs (filled square) were applied into laser-treated skin for indicated times in mice receiving FITC intravenously. Each symbol represents one array consisting of 9 MNs. The cutoff value is indicated by a dashed line and defined as Figure 1D. Inset shows fluorescence images of one anti-FITC-MN array. Note, all MNs in the array show uniform and strong FITC binding. Scale=100 μm. (B). The amounts of circulating FITC measured by anti-FITC-MNs are similar to those obtained with fluorescence

spectrophotometer. Anti-FITC-MNs or C-MNs were inserted into laser-treated skin for 30 min in mice receiving varying amounts of FITC intravenously, and the FITC captured on MNs was calculated by FITC intensity in comparison with a standard curve run in parallel.

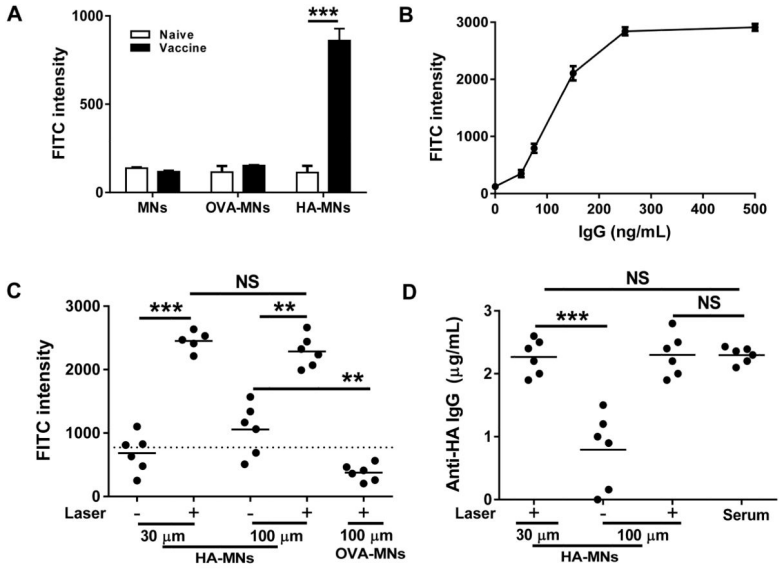

Fig. 4.

Measurement of anti-HA IgG in immunized mice. (A) Fluorescence intensity analysis demonstrates specific binding of anti-HA IgG to HA-MNs, but not to OVA-MNs in serum from immunized mice or naive mice. (B) A standard curve of FITC intensity on HA-MNs vs. known concentrations of anti-HA IgG. (C) Specific and sensitive capture of circulating anti-HA IgG in immunized mice. HA-MNs of 30 μm or 100 μm in length were inserted into laser-treated skin for 30 min. The MNs were removed and incubated with FITC–conjugated secondary antibody. FITC intensity was measured as (A). OVA-MNs of 100 μm in length were inserted into laser-treated skin by a procedure similar as negative controls. A dashed horizontal line is a cutoff value for positive FITC binding on the array as defined in Figure 1D. (D) A comparison of the concentrations of circulating anti-HA IgG measured by HA-MNs at different lengths in the presence or absence of laser treatment, as well as by a conventional IF assay of the corresponding serum (serum). n=6.

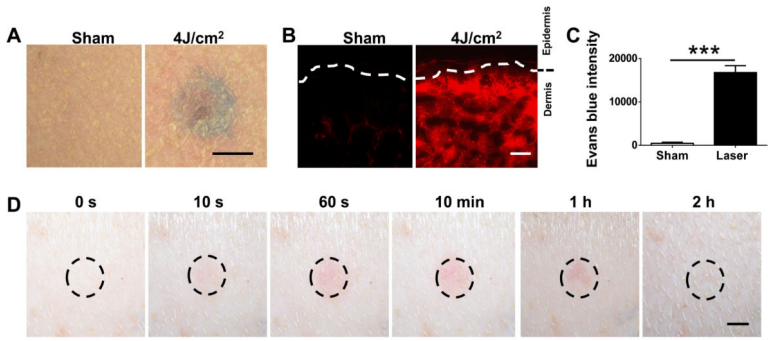

Fig. 5.

Extravasation and skin reaction after treating swine with a long pulse 595 nm laser. (A) Photos showing Evans blue dye leakage in laser-irradiated skin as compared to non-laser treated skin. (B&C) Increases in Evans blue fluorescence in laser-irradiated dermis (B) and in fluorescence intensity in the upper dermis in comparison with non-irradiated counterpart (C). (D) Skin reactions at indicated times after subject to 595 nm laser at 4 J/cm^2. Scale=5 mm in (A) and (D) or 100 μm in (B).

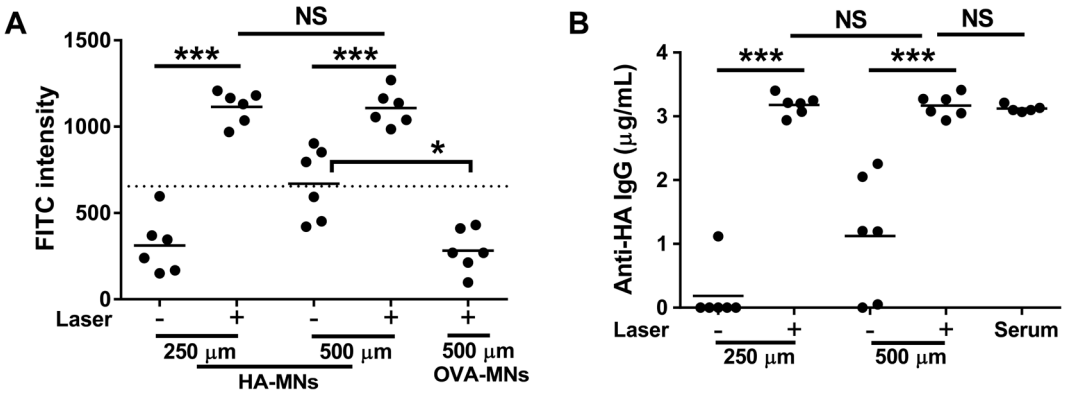

Fig. 6.

Measurement of anti-HA IgG in immunized pigs. (A) The amount of anti-HA IgG captured in the upper dermis was comparable to that in deep dermis after laser illumination. A dashed horizontal line is a cutoff value for positive FITC binding on the array as defined in Figure 1D. (B) The amount of anti-HA IgG in the upper dermis or dermis detected by MNs was similar to that in serum samples measured by conventional IF assays (serum).

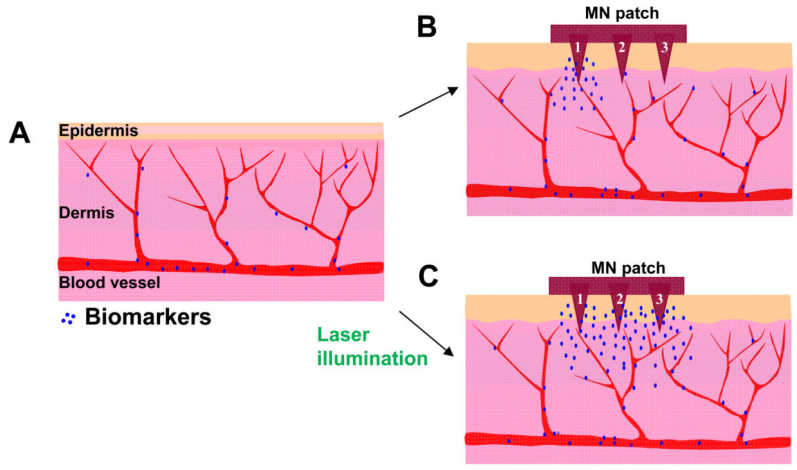

Fig. 7.

Schematic illustration of differences in distribution and concentration of circulating biomarkers in laser-treated and non-treated skins. (A) The skin without laser treatment. (B) Strong capture of circulating biomarkers occurs only on a MN that is physically close to a damaged capillary vessel like MN#1, but not on a MN that is away from an injured vessel like MN#3 in the absence of laser treatment. (C) In contrast, all MNs on the array are exposed to uniformly high concentrations of circulating biomarkers in laser-treated skin owing to laser-induced extravasation.